ACS APPLIED MATERIALS & INTERFACES

Research Article

www.acsami.org

Systematic Reliability Study of Top-Gate p- and n-Channel Organic Field-Effect Transistors

Do Kyung Hwang,[†,‡] Canek Fuentes-Hernandez,[†] Mathieu Fenoll,[†,§] Minseong Yun,[†] Jihoon Park,[⊥] Jae Won Shim,[†] Keith A. Knauer,[†] Amir Dindar,[†] Hyungchul Kim,[#] Yongjin Kim,[#] Jungbae Kim,[†] Hyeunseok Cheun,[†] Marcia M. Payne,[∥] Samuel Graham,[#] Seongil Im,[⊥] John E. Anthony,[∥] and Bernard Kippelen*[,†]

[†]Center for Organic Photonics and Electronics (COPE), School of Electrical and Computer Engineering, Georgia Institute of Technology, Atlanta, Georgia 30332-0250, United States

[‡]Interface Control Research Center, Future Convergence Research Technology Division, Korea Institute of Science and Technology (KIST), Seoul 136-791, South Korea

[§]Solvay SA, rue de Ransbeek 310, 1120 Brussels, Belgium

[⊥]Institute of Physics and Applied Physics, Yonsei University, Seoul 120-749, South Korea

[#]Center for Organic Photonics and Electronics (COPE), Woodruff School of Mechanical Engineering, Georgia Institute of Technology, Atlanta, Georgia 30332-0400, United States

[∥]Department of Chemistry, University of Kentucky, Lexington, Kentucky 40506, United States

Supporting Information

ABSTRACT: We report on a systematic investigation on the performance and stability of p-channel and n-channel top-gate OFETs, with a CYTOP/Al_2O_3 bilayer gate dielectric, exposed to controlled dry oxygen and humid atmospheres. Despite the severe conditions of environmental exposure, p-channel and n-channel top-gate OFETs show only minor changes of their performance parameters without undergoing irreversible damage. When correlated with the conditions of environmental exposure, these changes provide new insight into the possible physical mechanisms in the presence of oxygen and water. Photoexcited charge collection spectroscopy experiments provided further evidence of oxygen and water effects on OFETs. Top-gate OFETs also display outstanding durability, even when exposed to oxygen plasma and subsequent immersion in water or operated under aqueous media. These remarkable properties arise as a consequence of the use of relatively air stable organic semiconductors and proper engineering of the OFET structure.

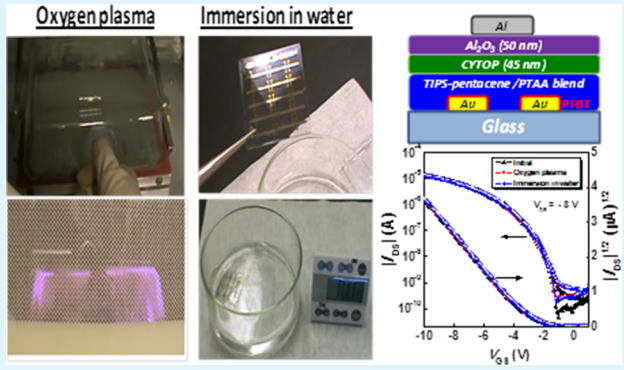

KEYWORDS: *organic electronics, organic field-effect transistors, soluble organic semiconductor, CYTOP/Al_2O_3 bilayer dielectric, device reliability, photoexcited charge collection spectroscopy*

INTRODUCTION

The science and technology of organic field-effect transistors (OFETs) have progressed significantly in recent years. OFETs are now processed from solution and display field-effect mobility values that are larger than those found in amorphous-silicon (*a*-Si) field-effect transistors.[1−6] Prototypes of electronic applications, such as drivers for flat-panel displays,[7−10] complementary circuits,[2,10−12] and various sensors,[8,13,14] have already been demonstrated. The improved air stability of the new generation of organic semiconductors[15−20] and advances in the optimization of the device geometries and material composition,[3,5,21,22] have also lead to OFETs that can operate in air for increasingly longer periods of time. As OFET technology is maturing, device reliability, namely the device's long-term environmental and operational stabilities, is a critical aspect that needs to be understood and optimized. A refined understanding of the device reliability is critical for the transition of academic technology into commercial applications.[23]

Compared to other species, oxygen and water are the most common reactive components in ambient air.[23] Isolating the individual effects of oxygen and water on the stability of an OFET is therefore critical to understanding the origin of the overall changes experienced by an OFET operating in air or in

Received: November 27, 2013
Accepted: February 13, 2014
Published: February 13, 2014

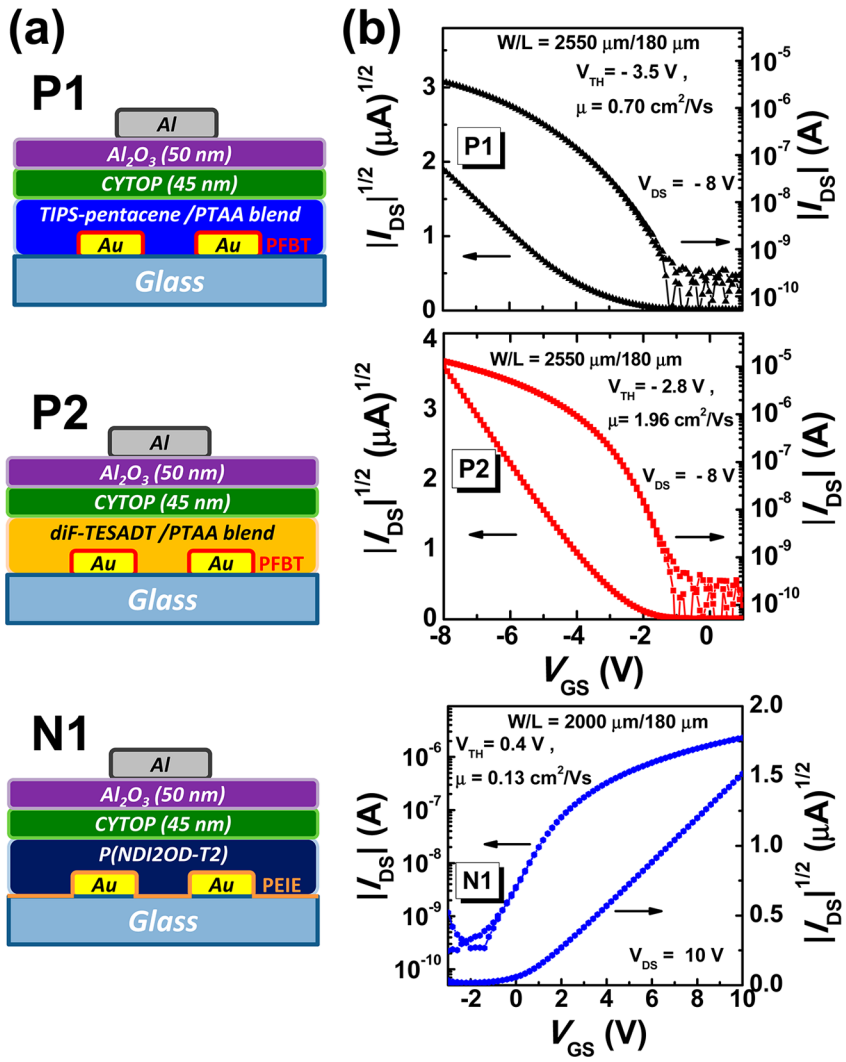

Figure 1. (a) Schematic cross-sectional view of **P1**, **P2**, and **N1** type OFETs. (b) Representative transfer characteristics plots of **P1**, **P2** (W/L = 2550 μm/180 μm), and **N1** type OFETs (W/L = 2000 μm/180 μm).

an aqueous environment. These changes arise as oxygen and water molecules in the environment diffuse into the OFET structure causing physical and/or chemical interactions that modify its electrical properties. For instance, oxygen and water molecules can cause oxidation of the organic active layer or metal electrodes, induce the creation of trap sites at grain boundaries or interfaces, or contribute to polarization of the gate dielectric layer.[23−29] Furthermore, prolonged exposure of an OFET to a reactive atmosphere commonly leads to irreversible damage to the organic semiconductor, the dielectric or the metallic layers that comprise its structure, making it difficult to conduct systematic studies.

Changes in the electrical properties of an OFET are reflected in changes to its field-effect mobility (μ), threshold voltage (V_{th}), on/off current ratio (I_{on}/I_{off}), and/or on the capacitance density of the gate dielectric (C_{in}). A clear identification of the physical or chemical origin of these changes is extremely difficult because they arise not only from extrinsic, but also from intrinsic factors that impact the OFET structure. In addition, these changes can manifest themselves on different time scales and can arise from very small electrical disturbances across the materials and interfaces of an OFET, which are otherwise hard to measure independently. Therefore, in order to study the extrinsic effects affecting the reliability of an OFET it is preferable to start with relatively stable devices.

Top-gate OFETs with a bilayer gate dielectric present a unique opportunity for the systematic study of the intrinsic and extrinsic degradation mechanisms in an OFET because they present good operational and environmental stability.[5,21,30] OFETs with this geometry display electrical properties that are stable for years in air, under continuous operation and can even sustain an oxygen plasma treatment. These properties arise as a consequence of using a carefully engineered bi-layer gate dielectric comprising a first amorphous fluoropolymer layer (such as CYTOP) having a low dielectric constant (k) and a second Al_2O_3 layer, a high-k metal-oxide, fabricated by atomic layer deposition (ALD). Here, we present a systematic investigation of the stability of p-channel and n-channel top-gate OFETs with a bilayer gate dielectric exposed to different reactive environments: dry oxygen (at 50 °C), air with an 80% relative humidity (at 50 °C), and pure water through immersion. We demonstrate that these OFETs display outstanding environmental stability and do not suffer irreversible damage from being subjected to these severe conditions. We also demonstrate stable operation of an OFET under water without suffering any degradation of its perform-

dx.doi.org/10.1021/am405424k | ACS Appl. Mater. Interfaces 2014, 6, 3378−3386

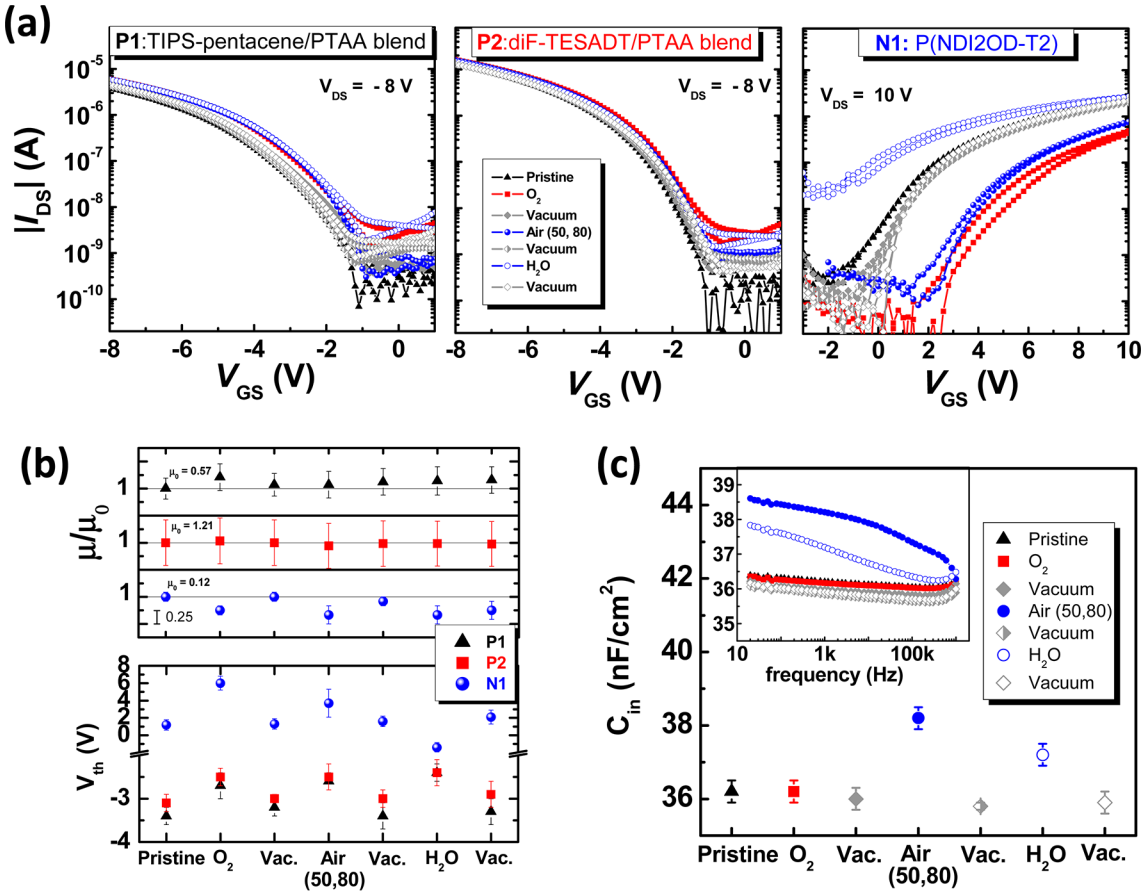

Figure 2. Environmental stability. (a) Transfer characteristics of **P1**, **P2**, and **N1** type OFETs measured after different conditions of environmental exposure. (b) The normalized average values of mobility, in the saturation region, and threshold voltage as a function of exposure sequences. (c) Variations in the averaged capacitance density as a function of exposure sequences and capacitance–frequency characteristics after undergoing exposure sequence (inset).

ance. These studies provide a consistent picture of the effects that oxygen and water have on the properties of p-channel and n-channel OFETs and allow a better understanding of the physical mechanisms affecting their long-term environmental and operational stability.

EXPERIMENTAL SECTION

Device Fabrication. OFETs with a bottom-contact and top-gate structure were fabricated on glass substrates (Corning Eagle2000) using p-channel and n-channel organic semiconductors as shown in Figure 1a. Thin-films of a blend of poly(triarylamine) (PTAA) and a soluble acene, 6,13-bis(triisopropylsilylethynyl) pentacene (TIPS-pentacene) or 2,8-difluoro-5,11-bis(triethylsilylethynyl) anthradithiophene (diF-TESADT), were used as the semiconductor in p-channel OFETs. Hereafter OFETs based on TIPS-pentacene and diF-TESADT will be referred to as **P1** and **P2**, respectively. An inkjet printed layer of poly[N,N′-bis(2-octyldodecyl)-naphthalene-1,4:5,8-bis(dicarboximide)-2,6-diyl]-alt-5,5′-(2,2′-bithiophene) [P(NDI2OD-T2), also called N2200] was used as the semiconductor in n-channel OFETs. Hereafter OFETs based on P(NDI2OD-T2) will be referred to as **N1**. For p-channel OFETs, a self-assembled monolayer of pentafluorobenzenethiol (PFBT) was formed on the Au electrodes by immersion in a 10 mM PFBT solution in ethanol for 15 min in a nitrogen-filled drybox, rinsing with pure ethanol, and drying. Soluble acenes: **P1** and **P2** and PTAA were blended in solutions prepared as follows: soluble acenes and PTAA were individually dissolved in 1,2,3,4-tetrahydronaphthalene anhydrous, 99%, (Sigma Aldrich) at a concentration of 30 mg/mL; solutions of one soluble acene (**P1** or **P2**) and PTAA were mixed at a weight ratio of 1:1. Blends of **P1**/PTAA and **P2**/PTAA were deposited by spin coating at 500 rpm for 10 s and at 2000 rpm for 20 s. Then, samples were annealed at 100 °C for 15 min in a nitrogen-filled drybox. For n-channel OFETs, a coating of polyethylenimine, 80% ethoxylated (PEIE) (M_w = 70 000 g/mol) was applied to the surface of the Au source and drain electrodes.[31] PEIE was dissolved in H_2O with a concentration of 35-40 wt.% when received from Aldrich. Then it was further diluted with 2-methoxyethanol to a weight concentration of 0.04 wt %. The solution was spin coated on top of the Au source and drain electrodes at a speed of 5000 rpm for 1 min and an acceleration of 1000 rpm/s. Spin-coated PEIE films were annealed at 100 °C for 10 min on a hot plate in ambient air. P(NDI2OD-T2) (Polyera ActivInk N2200), **N1**, was used as the n-channel semiconductor. **N1** ink was prepared as follows: **N1** was dissolved in mixture of 1,2,3,4-tetrahydronaphthalene anhydrous, 99% (Sigma, Aldrich) and mesitylene, 99% (Sigma Aldrich), with a ratio of 1:1 in volume in order to reach a 5 mg/mL concentration. A Dimatix DMP 2831 inkjet printing system was used to pattern the **N1** layer. A 100 nm thick layer of active material was printed in air at room temperature and annealed at 100 °C for 15 min in air. CYTOP (45 nm)/Al_2O_3 (50 nm) bilayers were used as top-gate dielectrics. CYTOP solution (CTL-809M) was purchased from Asahi Glass with a concentration of 9 wt %. To deposit a 45 nm thick film, we further diluted the original solution in CT-solv.180 (the original solvent) to have solution:solvent ratios of 1:3.5 in volume. 45 nm-thick CYTOP layers were deposited by spin-casting at 3000 rpm for 60 s. The CYTOP films were annealed at 100 °C for 20 min. Then, the Al_2O_3 dielectric films (50 nm) were deposited on top of the CYTOP layer using a Savannah 100 ALD system from Cambridge Nanotech Inc. Films were grown at 110 °C using alternating exposures of trimethyl aluminum [$Al(CH_3)_3$] and H_2O vapor at a deposition rate of

dx.doi.org/10.1021/am405424k | ACS Appl. Mater. Interfaces 2014, 6, 3378–3386

approximately 0.1 nm per cycle. Finally, Al (150 nm) gate electrodes were deposited by thermal evaporation through a shadow mask.

Electrical Characterization. Electrical characterization of the OFETs was carried out in a nitrogen-filled glove box (O_2, H_2O < 1 ppm). All current−voltage (I−V) characteristics of OFETs were measured with an Agilent E5272A source/monitor instrument.

Reliability Characterization. To investigate oxygen and water effects on device reliability, OFETs were exposed to six different ambient conditions as follows: dry oxygen ambient at 50 °C for 1 day, vacuum annealing at 100 °C for 16 h, humid air with relative humidity of 80% at 50 °C for 1 day, vacuum annealing at 100 °C for 16 h, immersion in distilled water for 16 h, and vacuum annealing at 100 °C for 16 h. Dry oxygen ambient (filled with 99% O_2 gas) and vacuum annealing conditions were created using a vacuum drying oven system (Yamato ADP 21). An environmental humidity chamber (Cincinnati Sub-Zero Product Inc.) was used for humid air ambient with relative humidity of 80%. Distilled water was used for immersion. At each interval, each substrate was briefly transferred back into a nitrogen-filled glove box and then electrical measurements and bias stress tests were carried out.

Photoexcited Charge Collection Spectroscopy (PECSS). The system consists of a light source of 500 W Hg(Xe) arc lamp (Oriel), a grating monochromator covering the spectral range of 300−1000 nm, an optical fiber (core diameter of 200 mm) as an optical probe, and a semiconductor parameter analyzer (4155C, Agilent Technology). Under an intense monochromatic light, the transfer curves were obtained from the testing OFETs connected to the electrical measurement unit. The photo-induced ΔV_{th} [ΔV_{th} = V_{th} (incident photon energy, eV) − V_{th}^{Dark}] was measured. The ΔV_{th} can be converted to the excited charge (Q_e). Finally, the DOS profiles can be extracted from the differential of Q_e.

RESULTS AND DISCUSSION

Figure 1b displays transfer characteristics of representative pristine OFETs (W/L= 2550 μm/180 μm) measured under a nitrogen atmosphere. Transfer characteristics correspond to hysteresis cycles wherein the voltage was swept back-and-forth between the extremes of the gate voltage (V_G) range displayed in the figure. Pristine OFETs refer to the condition of devices right-after deposition of the top-gate electrode, having minimum exposure to ambient air. All pristine OFETs exhibit hysteresis-free electrical characteristics and operate at voltages lower than 10 V. Maximum saturation field-effect mobility (μ_{max}) values of 0.7 cm^2/(V s), 1.96 cm^2/(V s), and 0.13 cm^2/(V s) were found for devices **P1**, **P2**, and **N1**, respectively. An average μ value of 0.57 ± 0.11 cm^2/(V s), V_{th} of −3.4 ± 0.2 V and I_{on}/I_{off} of 1 × 10^4 were measured on 9 devices of type **P1**. On 7 devices of type **P2** an average μ value of 1.21 ± 0.51 cm^2/(V s), V_{th} = −3.1 ± 0.2 V, I_{on}/I_{off} = 1 × 10^5 were found. On 7 devices of type **N1**, an average μ value of 0.12 ± 0.01 cm^2/(V s), V_{th} = 1.2 ± 0.6 V, I_{on}/I_{off} = 1 × 10^4 were found. Output characteristics are reported in Figure S1 in the Supporting Information. Overall, the performance of pristine OFETs is comparable to state-of-the-art OFETs previously reported in the literature.[1−4]

Pristine OFETs and capacitors with structure: Al/bilayer gate dielectric/Au, were sequentially exposed to: (1) a dry oxygen atmosphere at 50 °C for 24 h; (2) vacuum annealed at 100 °C under a pressure of 1 Torr for 16 h; (3) air at 50 °C with a relative humidity (RH) of 80% (hereon referred to as air (50, 80)) for 24 h; (4) vacuum annealed at 100 °C under a pressure of 1 Torr for 16 h; (5) immersed in water at room temperature for 16 h; (6) vacuum annealed at 100 °C under a pressure of 1 Torr for 16 h. These harsh environmental exposure conditions were selected to give sufficient time for oxygen and water molecules to diffuse into the OFET structure. The electrical properties of OFETs and capacitors were evaluated after exposure to different atmospheres and being transferred into a nitrogen-filled glove box. Further details on the conditions of atmospheric exposure and electrical evaluation are given in the experimental section.

Figure 2a displays transfer characteristics of **P1**, **P2**, and **N1** type OFETs measured after different environmental exposure conditions. The normalized average values of μ, in the saturation region, and V_{th} are shown in Figure 2b. Measurements of C_{in}, in capacitor structures, as a function of frequency (f) and condition of environmental exposure are shown in Figure 2c. C_{in} values measured after each condition of exposure were taken into account to calculate the values of μ presented in Figure 2b.

Different environmental exposure conditions induce small but nonetheless evident changes of $C_{in}(f)$ when the data is analyzed in detail. In capacitors that have undergone vacuum annealing $C_{in}(f)$ values are slightly smaller compared to values found in pristine or oxygen exposed capacitors, indicating that oxygen produces very small (<1%) but measurable increases of the magnitude of $C_{in}(f)$ without dramatically affecting its dispersion characteristics. We should note that although the bilayer gate dielectric (CYTOP/Al_2O_3) has been found to have relatively good encapsulation properties with an effective water vapor transmission rate of 1.1 × 10^{-3} g/m^2/day determined by a Ca test (see Figure S2 in the Supporting Information), oxygen in particular, is expected to diffuse through the bilayer gate dielectric after prolonged exposure. In contrast, capacitors exposed to humid atmospheres (air (50, 80) or immersed in H_2O) show larger $C_{in}(f)$ values and dispersive characteristics in the range from 20 Hz to 1 MHz. These changes of $C_{in}(f)$ are reversible upon vacuum annealing and attributed to the adsorption of water molecules in the gate dielectric; primarily in the Al_2O_3 layer. The dispersion characteristics can be explained by considering that mobile adsorbed dipolar water molecules can orient and polarizes the Al_2O_3 layer, resulting in increased C_{in} values at lower frequencies. At higher frequencies, the ability of these molecules to follow the external field decreases, resulting in a reduction of the values of $C_{in}(f)$. The adsorption of water in CYTOP is less likely because of its hydrophobic nature (contact angle is over 100°). Indeed, when single CYTOP layers (700 and 870 nm) undergo the same conditions of environmental exposure as the previously described capacitors, the values of $C_{in}(f)$ remain constant (see Figure S3 in the Supporting Information).

Taking changes of $C_{in}(f)$ into consideration, small and reversible variations of the average value of μ were observed in all types of OFETs when exposed to oxygen and/or humid atmospheres. These changes can be attributed to changes in the transport properties of the organic semiconductor layer and to changes in the contact resistance. **P1** and **P2** type OFETs display very stable average values of μ, with variations that in general are smaller than device-to-device variations (Figure 2b). This is consistent with the good electrochemical stability of these soluble acenes,[32] attributed primarily to the role of the bulky silylethynyl groups, at 6, 13 positions of TIPS-pentacene and at 5, 11 positions of diF-TESADT, in sterically hindering the irreversible oxidation of the molecules[33] and in mitigating the acenes' ability to assist in the formation of reactive singlet oxygen.[34] **N1** OFETs display slightly larger changes on the average values of μ but these changes are largely reversible after the devices undergo vacuum annealing. Further details on the changes of electrical performance parameters, square root

transfer and output characteristics after each step of the exposure sequence are summarized in Table S1 and Figure S4−S6 in the Supporting Information.

Observed changes of μ and V_{th} are consistent with the oxidation or reduction of oxygen and water molecules diffused into the semiconductor channel. For p-channel OFETs, oxygen exposure results in small increases of the average values of μ, reduced values of V_{th} and increased off-current values, I_{off}. Reduced values of V_{th} and increased I_{off} values have been reported in the past in air-exposed p-channel OFETs and rationalized as oxygen doping of the semiconductor channel.[25,26,33,35] An oxidation event (an electron transfer from an acene to an oxygen molecule) will lead to a hole being injected into the transport manifold and consequently to an increased charge density and channel conductivity.[25,26,33] The increased values of I_{off} observed in the transfer characteristics of **P1** and **P2** type OFETs after exposure to oxygen can be attributed to increased channel conductivity or to increased source to gate leakage current. We favor the first of these hypotheses because on **N1** type OFETs similar exposure to oxygen leads to the opposite trend, a reduction of I_{off}, indicating that changes of I_{off} are better correlated with changes in the electrical properties of the channel rather than with potential changes on the bilayer gate dielectric. The reduction of the values of V_{th} could arise directly from the oxidation of acene molecules around the contacts. An increased acene cation density will increase the Fermi level and bring it closer to the highest occupied molecular orbital (HOMO) edge, presumably making it easier for holes to be injected[36] by decreasing the width of the depletion region around the contact, reducing the contact resistance.[37] The reduction of the contact resistance is also consistent with the small increase in the average values of μ observed in **P1** and **P2** type OFETs after oxygen exposure. In the presence of water, **P2** type OFETs display remarkable stability with no change in the average values of μ. For **P1** type OFETs the average values of μ slightly increase after each exposure condition but variations remain within the range of device-to-device variations. The reduced values of V_{th} and increased values of I_{off} observed after exposure to humid atmospheres are similar to the ones observed after oxygen exposure. The influence of oxygen cannot be entirely ruled out after exposure to any of the humid atmospheres studied, considering that oxygen dissolved in water is present at part per million levels. However, it is very likely that, after immersion in water, shifts of V_{th} are driven primarily by dipolar water molecules diffused into the gate dielectric. The orientation of these dipolar molecules will increase the effective gate voltage and produce an apparent reduction of the value of V_{th}. As shown in Figure 2a, it is worth noting that none of these effects leads to hysteresis within the time frame the transfer characteristics of **P1** and **P2** type OFETs were acquired (a few minutes).

In **N1** type OFETs, oxygen and water molecules can be easily reduced at the semiconductor channel, therefore acting as electron traps.[38] Trapped charges can reduce the average values of μ due to an increased contact resistance arising from the decreased channel conductivity. These effects could also lead to the decreased values of I_{off} and the increased value of V_{th} observed after oxygen exposure and air (50, 80). Interestingly, V_{th} follows the opposite trend (V_{th} is reduced) after **N1** type OFETs are immersed in water. The reduction of V_{th} can be explained if we consider that as we have previously described, shifts of V_{th} could also arise because diffused water molecules could increase the effective gate voltage leading to excess holes or electrons and resulting in effective reductions of the value of V_{th}, revealed as positive shifts of V_{th} on p-channel and negative shifts of V_{th} for n-channel OFETs, as shown in Figure 2a, b. It is to be noted that as previously described, after exposure to air (50, 80), a positive shift of V_{th} was observed in **N1** type OFETs. In air (50, 80), the presence of oxygen is unavoidable so the shift of V_{th} must be a combination of the shifts induced by oxygen and water "alone". Indeed, if we take the average values of V_{th}, we can calculate the following shifts after oxygen exposure: (1) $\Delta V_{th}^{oxygen} = V_{th}^{oxygen} - V_{th}^{pristine} = 6.0\ V - 1.2\ V = 4.8\ V$ (positive shift); after water immersion: (2) $\Delta V_{th}^{water} = V_{th}^{water} - V_{th}^{pristine} = -1.4\ V - 1.2$ pristineV $= -2.6\ V$ (negative shift); and therefore, after exposure to air (50, 80), we can expect: (3) $\Delta V_{th}^{air(50,80)} = \Delta V_{th}^{oxygen} + \Delta V_{th}^{water} = 4.8\ V - 2.6\ V = 2.2\ V$ (positive shift), which yields a calculated $V_{th}^{air(50, 80)} = V_{th}^{pristine} + \Delta V_{th}^{air(50, 80)} = 1.2\ V + 2.2\ V = 3.4\ V$, which is similar to the value of 3.7 V measured in **N1** type OFETs. Finally, it is worth pointing out that, in contrast to p-channel OFETs, oxygen and water exposure causes hysteresis in the transfer characteristics of **N1** type OFETs devices.

In addition to these "static" characteristics, after each exposure step, the operational stability of the OFETs was also evaluated through a direct current (DC) bias-stress test. This "dynamic" test is expected to reveal the presence of deeper traps and slower polarization effects that cannot be resolved during the rapid evaluation of the transfer characteristics as described in Fig 2a. Figure 3a−c show the temporal evolution, over a period of 10 min, of the I_{DS} measured in all OFETs normalized to its initial value. Through these experiments, it is clear that in general water plays a more critical role than oxygen in the degradation of I_{DS} during bias stress test. For **P1** and **P2** type OFETs, the effect of oxygen is negligible. Pristine, oxygen exposed and vacuum annealed p-channel OFETs display variations of I_{DS} smaller than 2%. For **N1** type OFETs, oxygen molecules can create deep electron trap states due to its high electronegativity, resulting in a decrease of I_{DS} of about 20%. In OFETs exposed to humid atmospheres, I_{DS} decreased by 10−15% for **P1** and **P2** type OFETs and 30−40% for **N1** type OFETs. Therefore, we can conclude that water molecules create deep trapping states when OFETs are subjected to continuous bias stress. Here we need to point out that this trapping mechanism is different from the increased polarization of the gate dielectric that arises as water molecules orient under a low frequency external field. This extra polarization can affect OFET performance in two ways, first by increasing I_{DS} through the prefactor $C_{in}\mu W/L$ and by reducing the values of V_{th} as previously described. The first effect increases C_{in} by no more than 6% (Figure 2c), and consequently, I_{DS} by a similar amount. The second effect will produce more pronounced increases of I_{DS} through decreased values of V_{th}. Neither of these effects is consistent with the observed degradation of I_{DS} over time after exposure to humid atmospheres and therefore reveals a different mechanism in which water can act as an electron and hole trap, presumably in the organic semiconductor layer. Here, it is also important to note that in all cases, vacuum annealing leads to water detrapping and restores the I_{DS} stability found in pristine or vacuum annealed devices. Further details on bias stress conditions and I_{DS} variations are summarized in Table S2 in the Supporting Information. The reversible nature of all changes observed after vacuum annealing confirms that the interactions of oxygen and water with the organic semiconductor molecules are not permanent,

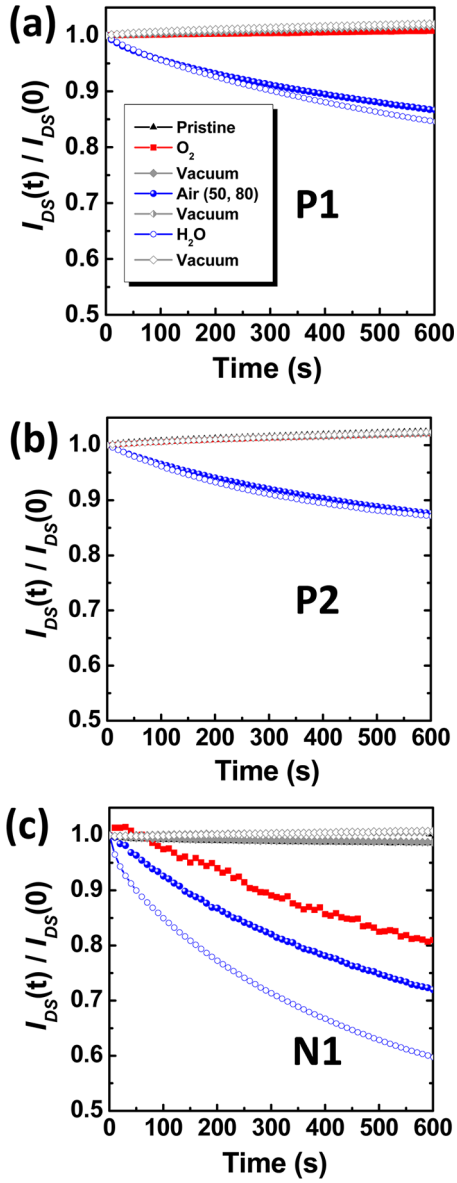

Figure 3. Operational stability. (a–c) Temporal evolution of the normalized drain current of **P1**, **P2**, and **N1** type OFETs under constant bias stress.

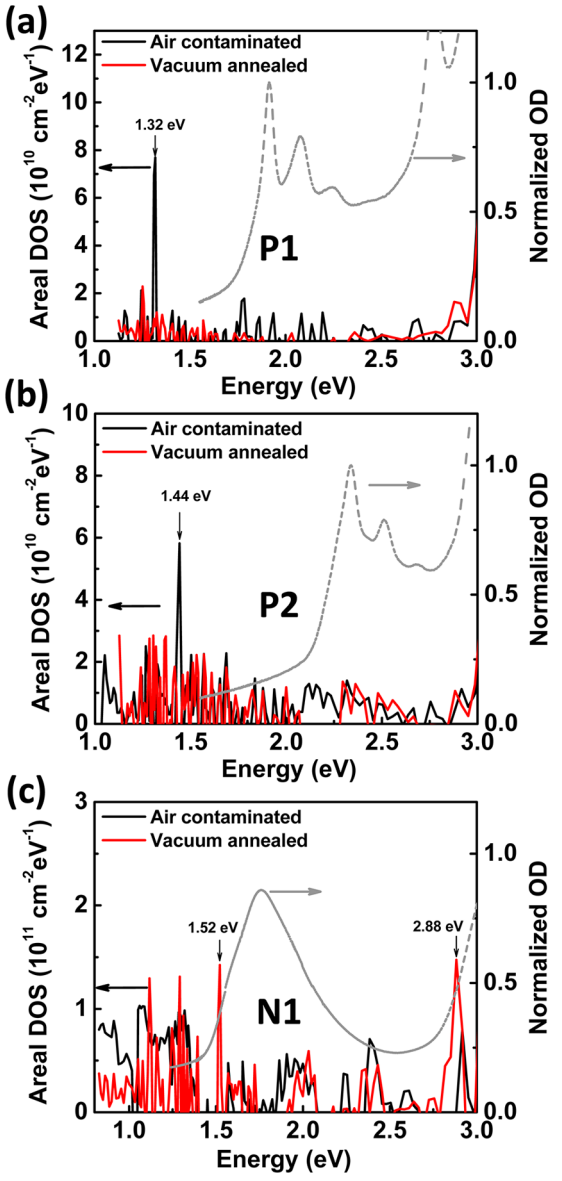

Figure 4. Density of state (DOS) profiles from photo excited charge collection spectroscopy (PECCS). (a, b) **P1** and **P2** OFETs. (c) **N1** type OFET. The optical absorption spectra on glass substrates are overlaid to be compared with the DOS profiles.

in these set of OFETs, because they can diffuse out of the device, leading to a performance that is similar to that found in pristine devices.

Photoexcited charge collection spectroscopy (PECCS), a type of charge modulation spectroscopy (CMS), allows for resolving the charge-induced absorption characteristics that can be directly correlated with charge excited quantum states of organic molecules. To further investigate the effects of environmental exposure on the behavior of top-gate OFETs, we conducted PECCS measurements. Details on the experimental method and extraction of the density of states (DOS) are given in the Experimental Section and previous studies.[39,40] Figure 4a–c displays the DOS profiles of ambient air exposed (a few weeks) and vacuum-annealed OFETs, wherein the charge-induced states in the DOS and the absorption spectra are overlaid to allow easy comparison. In **P1** and **P2** type OFETs, after ambient air exposure (oxygen and water), pronounced charge-induced peaks at 1.32 and 1.44 eV are observed in the DOS profiles, respectively (note that the peak at 1.32 eV in **P1** corresponds to a previously reported charge-induced peak position measured in TIPS-pentacene OFETs by CMS[41]). These charge induced peaks in the DOS profiles can be attributed to transitions between HOMO and singly occupied molecular orbital (SOMO) induced by acene cation states (hole charge carriers)[41] which are relevant for the positive shift of V_{th} and increased I_{off} currents observed in p-channel OFETs. After vacuum annealing, these charge induced signals in the DOS profiles were not detected. In contrast, in **N1** type OFETs no charge induced peaks were detected after air exposure, but after vacuum annealing, charge induced peaks at 1.52 and 2.88 eV were observed in the DOS profile. The position of these peaks are also well matched with previous peaks reported in **N1** measured by CMS.[42] Hence, these results correlate well with the interpretation of previous OFET characterization in that that oxygen and water lead to doping

dx.doi.org/10.1021/am405424k | ACS Appl. Mater. Interfaces 2014, 6, 3378–3386

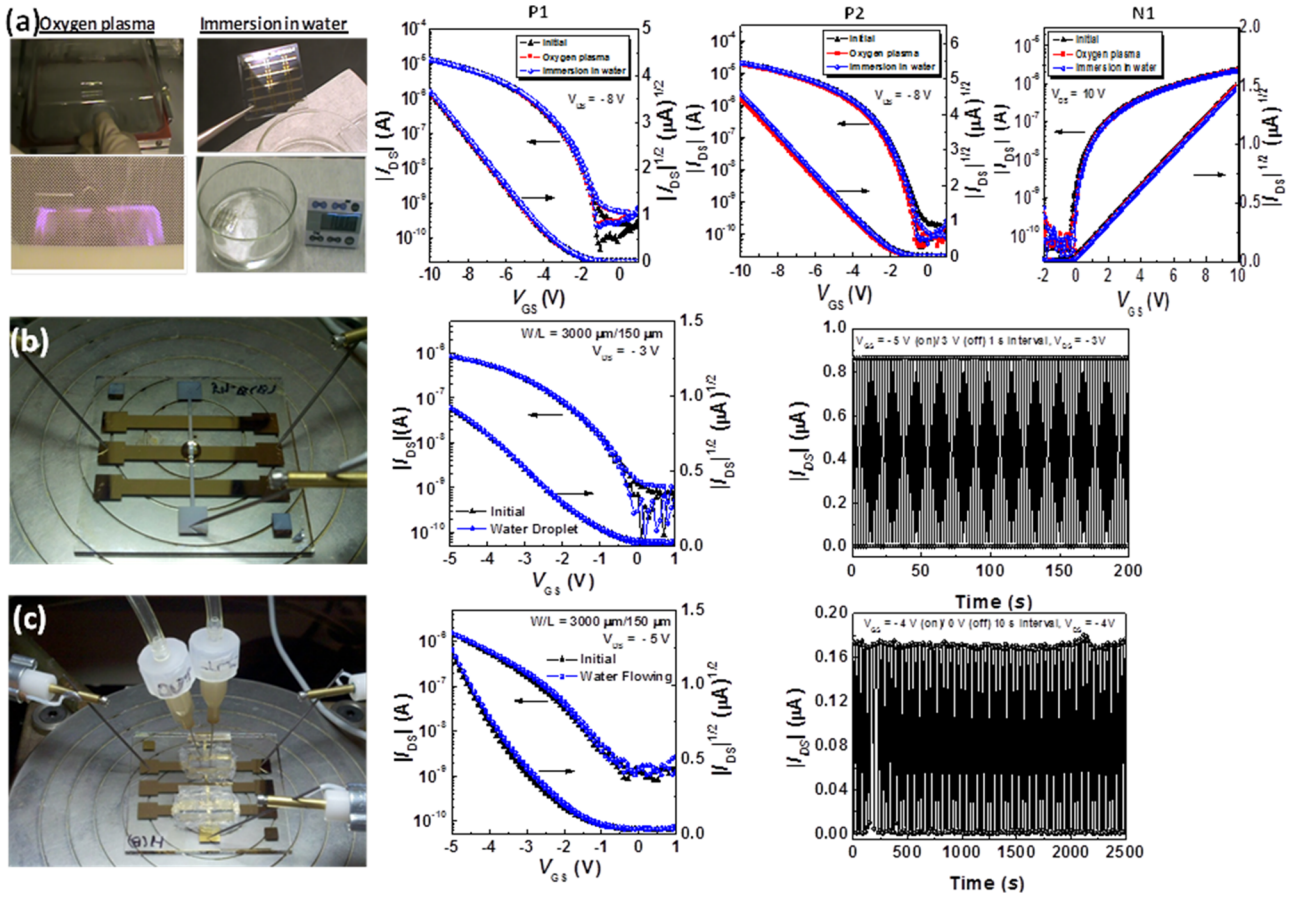

Figure 5. Device durability upon severe conditions of exposure. (a) Snapshot of device durability tests (O_2 plasma for 5 min and immersion in water for 1 h) and representative transfer characteristics of **P1**, **P2**, and **N1** type OFETs. (b) Photograph, transfer characteristics, and cycling test under water droplet of **P1** type OFET. (c) Photograph, transfer characteristics, and cycling test under water flowing of 0.6 μL/min of **P1** type OFET.

and trapping of charge carriers in *p*-channel and *n*-channel OFETs respectively.

Although we have seen changes in the parameters of p-channel and n-channel OFETs upon exposure to reactive oxygen and humid atmospheres, we should highlight the fact that the conditions of environmental exposure were rather severe. Under less stringent conditions, top-gate OFETs are remarkably stable and offer a stable platform for sensor applications. Detailed studies on the use of these top-gate OFETs as label-free chemical and biological sensors in aqueous environments will be published elsewhere.[43] Here, for completeness, we demonstrate the environmental stability of these OFETs by exposing them to oxygen plasma, and subsequently immersing them in water for 1 h. Figure 5a displays photographs illustrating these tests and demonstrates that the transfer characteristics of all types of OFETs, measured after this, present negligible variations after each condition of exposure. Furthermore, **P1** type OFETs where operated under a water droplet or under a flow of water (0.6 μL/min) covering the channel area. Here, we note that Ag or Au were used as top-gate electrodes instead of Al, to prevent its rapid oxidation. Figure 5b, c display the transfer characteristics and on/off I_{DS} currents cycling tests, wherein the OFET was subjected to several on- and off-gate voltage cycles at constant drain voltage, which demonstrate the outstanding environmental and operational stability of top-gate OFETs, even when operated in aqueous media.

CONCLUSIONS

We have presented a systematic investigation on the performance and stability of p-channel and n-channel top-gate OFETs, with a bilayer gate dielectric, exposed to controlled dry oxygen and humid atmospheres. Despite the severe conditions of environmental exposure, p-channel and n-channel top-gate OFETs show only minor changes of their performance parameters without undergoing irreversible damage. Very importantly, all changes where observed to be reversible after annealing the devices under vacuum. When changes of the performance parameters are correlated with the conditions of environmental exposure, it is revealed that oxygen acts as a dopant on p-channel OFETs, without compromising its stability under constant bias stress, and as a trap on n-channel OFETs. Water, on the other hand, not only polarizes the gate dielectric and decreases the threshold voltage of both types of OFETs, but under constant bias stress it can act as a deep trap severely degrading the performance of the OFETs. Photo-excited charge collection spectroscopy experiments provided further evidence of doping and charge trapping in p-channel and n-channel OFETs, respectively, in the presence of oxygen and water. Top-gate OFETs display outstanding durability, even when exposed to oxygen plasma and subsequent immersion in water. Although it is clear that the use of "air stable" organic semiconductors is critical to achieve this level of performance, this work underlines the critical importance of proper engineering of the OFET structure to maximize the potential for long term environmental and operational stability

dx.doi.org/10.1021/am405424k | ACS Appl. Mater. Interfaces 2014, 6, 3378−3386

of organic semiconductors. In particular, the ability of top-gate OFETs to show stable operation under aqueous media is expected to pave the way for the development of a new generation of chemical or biological sensors. We believe that the results presented will not only contribute toward developing a better understanding of the physical mechanisms affecting the long-term environmental and operational stability of OFETs but also toward developing novel device strategies to mitigate them.

■ ASSOCIATED CONTENT

Supporting Information

Pristine devices output characteristics, encapsulation property of CYTOP/Al_2O_3 bi-layer (water vapor transmission rate measurement), variations of capacitance density values of CYTOP single layer dielectrics as a function of exposure sequences, changes in the electrical performance parameters of μ and V_{th} and I_{DS} under bias stress tests of OFETs after undergoing exposure sequence. This material is available free of charge via the Internet at http://pubs.acs.org.

■ AUTHOR INFORMATION

Corresponding Author

*E-mail: kippelen@ece.gatech.edu. Phone: 404-385-5163.

Author Contributions

The manuscript was written through contributions of all authors. All authors have given approval to the final version of the manuscript.

Notes

The authors declare no competing financial interest.

■ ACKNOWLEDGMENTS

This material is based on work supported in part by Solvay S.A., by the Office of Naval Research through Contract Award N00014-04-1-0120 and N00014-11-1-0329, and by the STC Program of the National Science Foundation under Agreement DMR-0120967.

■ REFERENCES

(1) Giri, G.; Verploegen, E.; Mannsfeld, S. C. B.; Atahan-Evrenk, S.; Kim, D. H.; Lee, S. Y.; Becerril, H. A.; Aspuru-Guzik, A.; Toney, M. F.; Bao, Z. A. Tuning Charge Transport in Solution-Sheared Organic Semiconductors using Lattice Strain. *Nature* **2011**, *480*, 504−509.

(2) Yan, H.; Chen, Z. H.; Zheng, Y.; Newman, C.; Quinn, J. R.; Dotz, F.; Kastler, M.; Facchetti, A. A High-Mobility Electron-Transporting Polymer for Printed Transistors. *Nature* **2009**, *457*, 679−687.

(3) Hamilton, R.; Smith, J.; Ogier, S.; Heeney, M.; Anthony, J. E.; McCulloch, I.; Veres, J.; Bradley, D. D. C.; Anthopoulos, T. D. High-Performance Polymer-Small Molecule Blend Organic Transistors. *Adv. Mater.* **2009**, *21*, 1166−1171.

(4) Smith, J.; Zhang, W.; Sougrat, R.; Zhao, K.; Li, R.; Cha, D.; Amassian, A.; Heeney, M.; McCulloch, I.; Anthopoulos, T. D. Solution-Processed Small Molecule-Polymer Blend Organic Thin-Film Transistors with Hole Mobility Greater than 5 cm^2/V s. *Adv. Mater.* **2012**, *24*, 2441−2446.

(5) Hwang, D. K.; Fuentes-Hernandez, C.; Kim, J.; Potscavage, W. J.; Kim, S. J.; Kippelen, B. Top-Gate Organic Field-Effect Transistors with High Environmental and Operational Stability. *Adv. Mater.* **2011**, *23*, 1293−1298.

(6) Hwang, D. K.; Fuentes-Hernandez, C.; Berrigan, J. D.; Fang, Y. N.; Kim, J.; Potscavage, W. J.; Cheun, H.; Sandhage, K. H.; Kippelen, B. Solvent and Polymer Matrix Effects on TIPS-Pentacene/Polymer Blend Organic Field-Effect Transistors. *J. Mater. Chem.* **2012**, *22*, 5531−5537.

(7) Zhou, L. S.; Wanga, A.; Wu, S. C.; Sun, J.; Park, S.; Jackson, T. N. All-Organic Active Matrix Flexible Display. *Appl. Phys. Lett.* **2006**, *88*, 083502.

(8) Sekitani, T.; Someya, T. Stretchable, Large-area Organic Electronics. *Adv. Mater.* **2010**, *22*, 2228−2246.

(9) Sekitani, T.; Nakajima, H.; Maeda, H.; Fukushima, T.; Aida, T.; Hata, K.; Someya, T. Stretchable Active-Matrix Organic Light-Emitting Diode Display using Printable Elastic Conductors. *Nat. Mater.* **2009**, *8*, 494−499.

(10) Gelinck, G.; Heremans, P.; Nomoto, K.; Anthopoulos, T. D. Organic Transistors in Optical Displays and Microelectronic Applications. *Adv. Mater.* **2010**, *22*, 3778−3798.

(11) Klauk, H.; Zschieschang, U.; Pflaum, J.; Halik, M. Ultralow-Power Organic Complementary Circuits. *Nature* **2007**, *445*, 745−748.

(12) Zhang, X. H.; Potscavage, W. J.; Choi, S.; Kippelen, B. Low-Voltage Flexible Organic Complementary Inverters With High Noise Margin and High Dc Gain. *Appl. Phys. Lett.* **2009**, *94*, 043312.

(13) Someya, T.; Dodabalapur, A.; Huang, J.; See, K. C.; Katz, H. E. Chemical and Physical Sensing by Organic Field-Effect Transistors and Related Devices. *Adv. Mater.* **2010**, *22*, 3799−3811.

(14) Sekitani, T.; Yokota, T.; Zschieschang, U.; Klauk, H.; Bauer, S.; Takeuchi, K.; Takamiya, M.; Sakurai, T.; Someya, T. Organic Nonvolatile Memory Transistors for Flexible Sensor Arrays. *Science* **2009**, *326*, 1516−1519.

(15) Kobayashi, N.; Sasaki, M.; Nomoto, K. Stable peri-Xanthenoxanthene Thin-Film Transistors with Efficient Carrier Injection. *Chem. Mater.* **2009**, *21*, 552−556.

(16) Zschieschang, U.; Ante, F.; Yamamoto, T.; Takimiya, K.; Kuwabara, H.; Ikeda, M.; Sekitani, T.; Someya, T.; Kern, K.; Klauk, H. Flexible Low-Voltage Organic Transistors and Circuits Based on a High-Mobility Organic Semiconductor with Good Air Stability. *Adv. Mater.* **2010**, *22*, 982−985.

(17) Zhao, Y.; Di, C. A.; Gao, X. K.; Hu, Y. B.; Guo, Y. L.; Zhang, L.; Liu, Y. Q.; Wang, J. Z.; Hu, W. P.; Zhu, D. B. All-Solution-Processed, High-Performance *n*-Channel Organic Transistors and Circuits: Toward Low-Cost Ambient Electronics. *Adv. Mater.* **2011**, *23*, 2448−2453.

(18) Glowacki, E. D.; Irimia-Vladu, M.; Kaltenbrunner, M.; Gasiorowski, J.; White, M. S.; Monkowius, U.; Romanazzi, G.; Suranna, G. P.; Mastrorilli, P.; Sekitani, T.; Bauer, S.; Someya, T.; Torsi, L.; Sariciftci, N. S. Hydrogen-Bonded Semiconducting Pigments for Air-Stable Field-Effect Transistors. *Adv. Mater.* **2013**, *25*, 1563−1569.

(19) Cho, H.; Lee, S.; Cho, N. S.; Jabbour, G. E.; Kwak, J.; Hwang, D. H.; Lee, C. High-Mobility Pyrene-Based Semiconductor for Organic Thin-Film Transistors. *ACS Appl. Mater. Interfaces* **2013**, *5*, 3855−3860.

(20) Yokota, T.; Kuribara, K.; Tokuhara, T.; Zschieschang, U.; Klauk, H.; Takimiya, K.; Sadamitsu, Y.; Hamada, M.; Sekitani, T.; Someya, T. Flexible Low-Voltage Organic Transistors with High Thermal Stability at 250 °C. *Adv. Mater.* **2013**, *25*, 3639−3644.

(21) Hwang, D. K.; Dasari, R. R.; Fenoll, M.; Alain-Rizzo, V.; Dindar, A.; Shim, J. W.; Deb, N.; Fuentes-Hernandez, C.; Barlow, S.; Bucknall, D. G.; Audebert, P.; Marder, S. R.; Kippelen, B. Stable Solution-Processed Molecular *n*-Channel Organic Field-Effect Transistors. *Adv. Mater.* **2012**, *24*, 4445−4450.

(22) Lee, W. H.; Kwak, D.; Anthony, J. E.; Lee, H. S.; Choi, H. H.; Kim, D. H.; Lee, S. G.; Cho, K. The Influence of the Solvent Evaporation Rate on the Phase Separation and Electrical Performances of Soluble Acene-Polymer Blend Semiconductors. *Adv. Funct. Mater.* **2012**, *22*, 267−281.

(23) Sirringhaus, H. Reliability of Organic Field-Effect Transistors. *Adv. Mater.* **2009**, *21*, 3859−3873.

(24) De Angelis, F.; Gaspari, M.; Procopio, A.; Cuda, G.; Di Fabrizio, E. Direct Mass Spectrometry Investigation on Pentacene Thin Film Oxidation Upon Exposure to Air. *Chem. Phys. Lett.* **2009**, *468*, 193−196.

(25) Han, S. H.; Kim, J. H.; Jang, J.; Cho, S. M.; Oh, M. H.; Lee, S. H.; Choo, D. J. Lifetime of Organic Thin-Film Transistors with Organic Passivation Layers. *Appl. Phys. Lett.* **2006**, *88*, 073519.
(26) Jung, H.; Lim, T.; Choi, Y.; Yi, M.; Won, J.; Pyo, S. Lifetime Enhancement of Organic Thin-Film Transistors Protected with Organic Layer. *Appl. Phys. Lett.* **2008**, *92*, 163504.
(27) Qiu, Y.; Hu, Y. C.; Dong, G. F.; Wang, L. D.; Xie, J. F.; Ma, Y. N. H_2O Effect on the Stability of Organic Thin-Film Field-Effect Transistors. *Appl. Phys. Lett.* **2003**, *83*, 1644.
(28) Li, D. W.; Borkent, E. J.; Nortrup, R.; Moon, H.; Katz, H.; Bao, Z. N. Humidity Effect on Electrical Performance of Organic Thin-Film Transistors. *Appl. Phys. Lett.* **2005**, *86*, 042105.
(29) Jung, T.; Dodabalapur, A.; Wenz, R.; Mohapatra, S. Moisture Induced Surface Polarization in a Poly(4-Vinyl Phenol) Dielectric in an Organic Thin-Film Transistor. *Appl. Phys. Lett.* **2005**, *87*, 182109.
(30) Hwang, D. K.; Fuentes-Hernandez, C.; Kim, J. B.; Potscavage, W. J.; Kippelen, B. Flexible and Stable Solution-Processed Organic Field-Effect Transistors. *Org. Electron.* **2011**, *12*, 1108−1113.
(31) Zhou, Y.; Fuentes-Hernandez, C.; Shim, J.; Meyer, J.; Giordano, A. J.; Li, H.; Winget, P.; Papadopoulos, T.; Cheun, H.; Kim, J.; Fenoll, M.; Dindar, A.; Haske, W.; Najafabadi, E.; Khan, T. M.; Sojoudi, H.; Barlow, S.; Graham, S.; Bredas, J.-L.; Marder, S. R.; Kahn, A.; Kippelen, B. A Universal Method to Produce Low-Work Function Electrodes for Organic Electronics. *Science* **2012**, *336*, 327−332.
(32) Griffith, O. L.; Anthony, J. E.; Jones, A. G.; Lichtenberger, D. L. Electronic Properties of Pentacene versus Triisopropylsilylethynyl-Substituted Pentacene: Environment-Dependent Effects of the Silyl Substituent. *J. Am. Chem. Soc.* **2010**, *132*, 580−586.
(33) Park, S. K.; Mourey, D. A.; Han, J. I.; Anthony, J. E.; Jackson, T. N. Environmental and Operational Stability of Solution-Processed 6,13-Bis(Triisopropyl-Silylethynyl) Pentacene Thin Film Transistors. *Org. Electron.* **2009**, *10*, 486−490.
(34) Maliakal, A.; Raghavachari, K.; Katz, H.; Chandross, E.; Siegrist, T. Photochemical Stability of Pentacene and a Substituted Pentacene in Solution and in Thin Films. *Chem. Mater.* **2004**, *16*, 4980−4986.
(35) Klauk, H. *Organic Electronics: Materials, Manufacturing and Applications*; Wiley-VCH: Weinheim, Germany, 2006; Chapter 5.
(36) Lussem, B.; Riede, M.; Leo, K. Doping of Organic Semiconductors. *Phys. Status Solidi A* **2013**, *210*, 9−43.
(37) Tiwari, S. P.; Potscavage, W. J.; Sajoto, T.; Barlow, S.; Marder, S. R.; Kippelen, B. Pentacene Organic Field-Effect Transistors with Doped Electrode-Semiconductor Contacts. *Org. Electron.* **2010**, *11*, 860−863.
(38) Di Pietro, R.; Fazzi, D.; Kehoe, T. B.; Sirringhaus, H. Spectroscopic Investigation of Oxygen- and Water-Induced Electron Trapping and Charge Transport Instabilities in *n*-type Polymer Semiconductors. *J. Am. Chem. Soc.* **2012**, *134*, 14877−14889.
(39) Lee, K.; Oh, M. S.; Mun, S. J.; Lee, K. H.; Ha, T. W.; Kim, J. H.; Park, S. H. K.; Hwang, C. S.; Lee, B. H.; Sung, M. M.; Im, S. Interfacial Trap Density-of-States in Pentacene- and ZnO-Based Thin-Film Transistors Measured via Novel Photo-excited Charge-Collection Spectroscopy. *Adv. Mater.* **2010**, *22*, 3260−3265.
(40) Lee, J.; Lee, B. L.; Kim, J. H.; Lee, S.; Im, S. Photoexcited Charge Collection Spectroscopy of Two-Dimensional Polaronic States in Polymer Thin-Film Transistors. *Phys. Rev. B* **2012**, *85*, 045206.
(41) Sakanoue, T.; Sirringhaus, H. Band-like Temperature Dependence of Mobility in a Solution-Processed Organic Semiconductor. *Nat. Mater.* **2010**, *9*, 736−740.
(42) Caironi, M.; Bird, M.; Fazzi, D.; Chen, Z. H.; Di Pietro, R.; Newman, C.; Facchetti, A.; Sirringhaus, H. Very Low Degree of Energetic Disorder as the Origin of High Mobility in an *n*-Channel Polymer Semiconductor. *Adv. Funct. Mater.* **2011**, *21*, 3371−3381.
(43) Yun, M.; Sharma, A.; Fuentes-Hernandez, C.; Hwang, D. K.; Dindar, A.; Singh, S.; Choi, S.; Kippelen, B. Stable Organic Field-Effect Transistors for Continuous and Non-Destructive Chemical and Biological Sensing in Aqueous Environment. *ACS Appl. Mater. Interfaces* **2014**, DOI: 10.1021/am404460j.